T.D. Karaca et al / Hacettepe J. Biol. & Chem., 2025, 53 (4), 33-46

Research Article

Hacettepe Journal of Biology and Chemistry

journal homepage: https://hjbc.hacettepe.edu.tr/
Dergipark Akademik: https://dergipark.org.tr/en/pub/hjbc

Analyses and Comparisons of the Antimicrobial-Cytotoxic Effects and Molecular Docking Study of L-DOPA and L-DOPA Methyl Ester

L-DOPA ve L-DOPA Metil Esteri'nin Antimikrobiyal-Sitotoksik Etkilerinin ve Moleküler Yerleştirme Çalışmasının Analizleri ve Karşılaştırmaları

Tuğçe Deniz Karaca[1*], Hüseyin Balcı[2], Arzu Aysan[3], Yusuf Sert[4]

[1]Gazi University, Department of Medical Services and Techniques, Vocational School of Health Services, Ankara, Türkiye.
[2]Gebze Technical University, Department of Molecular Biology and Genetics, Kocaeli, Türkiye.
[3]Gebze Technical University, Department of Molecular Biology and Genetics, Kocaeli, Türkiye.
[4]Yozgat Bozok University, Department of Physics, Faculty of Art & Sciences, Yozgat, Türkiye.

ABSTRACT

The increasing the importance of synthesizing compounds with high biocompatibility, low cytotoxicity, and advanced antibacterial properties is evident in current research. L-3,4-Dihydroxyphenylalanine (L-DOPA) is a crucial drug widely used in the treatment of Parkinson's disease. In this study, we investigated the antimicrobial and cytotoxic effects of L-DOPA and its water-soluble derivative, L-DOPA methyl ester. The antimicrobial effects of L-DOPA and L-DOPA Methyl Ester were tested on both Gram-negative and Gram-positive bacteria. Additionally, the impact of L-DOPA and its ester on cell viability was assessed using the MTT assay on cancerous and non-cancerous cell lines. The study revealed that both substances were effective against Gram-positive bacteria but not Gram-negative bacteria. Specifically, the growth of Gram-positive bacteria was inhibited by both compounds, with L-DOPA showing greater efficacy. We also observed that L-DOPA and its ester exhibit anti-cancer activity. Furthermore, the molecular docking mechanism between the three targets (2DS2, 4URO and 1M17) and the compounds was investigated using Autodock Vina. The findings show that the L-DOPA molecule is more appropriately attached to the target receptors than the L-DOPA methyl ester molecule. As a result, its inhibition is greater. The results obtained are new and it is thought that these results of the study will contribute to the development of new synthesizable drug studies.

Key Words
L-Dopa-ester, antimicrobial activity, cytotoxicity, molecular docking.

ÖZ

Yüksek biyouyumluluk, düşük sitotoksisite ve gelişmiş antibakteriyel özelliklere sahip bileşiklerin sentezlenmesinin artan önemi güncel araştırmalarda açıkça görülmektedir. L-3,4-dihidroksifenilalanin (L-DOPA), Parkinson hastalığının tedavisinde yaygın olarak kullanılan önemli bir ilaçtır. Bu çalışmada, L-DOPA ve suda çözünür türevi L-DOPA metil esterinin antimikrobiyal ve sitotoksik etkilerini araştırdık. L-DOPA ve L-DOPA Metil Esterinin antimikrobiyal etkileri hem Gram negatif hem de Gram pozitif bakterilerde test edildi. Ek olarak, L-DOPA ve esterinin hücre canlılığı üzerindeki etkisi, kanserli ve kanserli olmayan hücre hatlarında MTT testi kullanılarak değerlendirildi. Çalışma, her iki maddenin de Gram pozitif bakterilere karşı etkili olduğunu ancak Gram negatif bakterilere karşı etkili olmadığını ortaya koydu. Özellikle, Gram pozitif bakterilerin büyümesi her iki bileşik tarafından da engellendi ve L-DOPA daha fazla etkinlik gösterdi. Ayrıca L-DOPA ve esterinin antikanser aktivite gösterdiğini gözlemledik. Ayrıca, üç hedef (2DS2, 4URO ve 1M17) ile bileşikler arasındaki moleküler yerleştirme mekanizması Autodock Vina kullanılarak araştırıldı. Bulgular, L-DOPA molekülünün hedef reseptörlere L-DOPA metil ester molekülünden daha uygun şekilde bağlandığını göstermektedir. Sonuç olarak, inhibisyonu daha fazladır. Elde edilen sonuçlar yenidir ve çalışmanın bu sonuçlarının yeni sentezlenebilir ilaç çalışmalarının geliştirilmesine katkıda bulunacağı düşünülmektedir.

Anahtar Kelimeler
L-Dopa-ester, antimikrobiyal aktivite, sitotoksisite, moleküler yerleştirme.

Article History: Apr 28, 2025; Accepted: Sep 10, 2025; Available Online: Sep 30, 2025.
DOI: https://doi.org/10.15671/hjbc.1684535
Correspondence to: T.D. Karaca, Gazi University, Department of Medical Services and Techniques, Vocational School of Health Services, Ankara, Türkiye.
E-Mail: tdenizkaraca@gazi.edu.tr

INTRODUCTION

Recently, widespread drug resistance against infectious bacterial pathogens and the impact of this situation on the treatment of diseases have become extremely important. This problem has made it necessary to investigate new generation agents from new sources. To date, several hundreds of antimicrobial agents have been discovered. However, much less than 1% of them have become drugs [1]. Structures of several dozen of known antibacterial, antifungal or antiprotozoal agents are based on the amino acid. In most of them, the amino acid skeleton is of a vitally importance for their biological activity. For this reason, amino acid-based some derivatives, which constitute a group of compounds with various biological activities, have found many applications in the medical fields because of their high level of biocompatibility and biodegradability [2]. And also, various drug discovery techniques allow the discovery of new different chemical entities with high pharmacological activities [3,4]. In chemical modifications, one of the several ways to increase the solubility and passive permeability of the parent drug in the traditional prodrug approach involves the introduction of lipophilic groups such as alkyl [5,6]. Therefore, research on the biological activities of alkyl esters of amino acid derivatives are interesting. However, there are very few studies in the literature on amino acid alkyl esters, which have been determined to have antibacterial and anticancer activities. In addition, a remarkable study found that some esters of dopamine, a phenolic compound derived from tyrosine, are have antibacterial activity [7-9]. Some studies also suggest that materials consisting of ester bonds between amino acids and polysaccharides are useful for targeted drug delivery, bioimaging or surface functionalization [10]. These compounds exhibit antimicrobial properties due to their ability to interact with the bacterial membrane [11-12].

L-3,4-Dihydroxyphenylalanine (L-DOPA) is an aromatic and a bioactive amino acid that produces dopamine in the body after oral ingestion. Commonly administered for symptom management in patients with Parkinson's disease. It is also emphasized in the literature that various DOPA-based derivatives show antiproliferative, antibacterial and antimicrobial activities. This is promising in terms of pharmacological effects [13-15]. Important results of various applications of ester prodrugs of L-DOPA are reported in the literature, but they are limited in number. These studies were conducted with Dopa esters with groups such as Octyl, Decyl, Dodecyl, Tetradecyl, and it was determined that the esters had antibacterial activity [16-18]. Additionally, only one study reported the in vivo antitumour activity of DOPA methyl ester [19]. L-DOPA methyl ester is a soluble neutral derivative of L-DOPA formulated for increased solubility compared to the parent compound. It is especially important to conduct research on water-soluble DOPA methyl ester, and such information is also needed for the synthesis of new biologically active compounds based on DOPA.

Therefore, in this study, antimicrobial activity and cytotoxicity studies of L-DOPA and L-DOPA methyl ester were performed, as well as molecular docking studies of the compounds and discussed comparatively. The results of the study are new data to the literature and will contribute to further research on DOPA derivatives and strengthen the development of new strategies using DOPA-based synthesizable molecules and contribute to advances in drug development research.

MATERIALS and METHODS

Chemicals

All the chemicals, reagents, and media supplements were purchased from Sigma-Aldrich (St. Louis, MO, USA), Merck (Darmstadt, Germany), Becton Dickinson and Company (Franklin Lakes, NJ, USA), and Gibco, Thermo Fisher Scientific (Waltham, MA, USA). The CellTiter 96® AQueous One Solution Cell Proliferation (MTS) Assay was provided by Promega (Madison, WI, USA). The human embryonic kidney cell line HEK293, undifferentiated human neuroblastoma SHSY5Y and the hepatocellular carcinoma cell lines PLC/PRF/5 and HuH7 were supplied by ATCC.

Minimum Inhibitory Concentration Assays

Using the modified microdilution broth method [20], the *in vitro* antibacterial activities of L-DOPA (LD) and L-DOPA Methyl Ester (LDME) were tested against Gram-positive *Staphylococcus aureus* ATCC 29213 and Gram-negative *Escherichia coli* ATCC 53323 in the 96-well microplates. The stock solution for compounds was made using distilled water. After being serially diluted with the growth medium, the final concentration varied from 3.9 mM to 4000 mM. Ampicillin and streptomycin, widely used antibiotics, were employed as positive controls at the same concentrations as the tested compounds. Additionally, growth controls without any

drugs were included. 100 ml of LB medium was added from the second well to the 12th well in each column on the 96-well microplate. To make a serial double dilution, 200 ml of the stock solution was added to the first wells in each column. Then, 100 ml were transferred from the first to the eleventh well. The 12th well was drug-free and used to control growth. Finally, 100 ml of the bacterial suspension was added to each well to obtain 10^{5}° cells/ml. The MIC values were calculated after 24 hours of incubation at 37°C in a humid atmosphere. The lowest concentration of compounds at which no growth was observed compared to the control was designated as the minimum inhibitory concentration (MIC). Using a Fluostar Omega Microplate Reader (BMG Labtech, Ortenberg, Germany), the results were also ascertained spectrophotometrically after being evaluated visually. Each concentration was tested in triplicate, and the entire procedure was repeated at least twice.

Biofilm Assay

First, bacteria from the frozen stock were streaked onto LB agar plates at -80°C. After that, the streaked plates were kept at 37 °C overnight to encourage bacterial growth. With the growing colonies onto streaked plates, a bacterial solution for *E. coli* and *S. aureus* was made in the media of Tryptic Soy Broth and Tryptic Soy Broth 66% supplemented with glucose 0.2%, respectively. The bacterial solution's OD value was set to 0.1 (OD600 = 0.1, i.e., 10^{8} CFU/ml). Each substance (LD and LDME) was put to a separate well of a 96-well plate in concentrations ranging from 3.9 to 4000 mM. The appropriate amount of the bacterial solution containing roughly 10^{8} CFU/ml of *E. coli* or *S. aureus* was then added to each well to obtain 10^{5} cells/ml, and the mixture was then incubated for 96 hours at 37°C without shaking. As controls, the drug-free wells were used. After the wells had been incubated, they were washed twice with distilled water to get rid of any adherent cells before being stained for 15 minutes at room temperature with 0.4% crystal violet. The leftover dye was then eluted by applying a 33% acetic acid solution for 15 minutes after three distilled water washes to the stained wells. Utilizing a Fluostar Omega Microplate Reader (BMG Labtech, Ortenberg, Germany) and absorbance at OD595, biofilm biomass was then calculated.

Cell Culture and Treatment Paradigm

Hepatocellular carcinoma (HCC) cell lines HUH7 and PLC/PRF/5, human embryonic kidney cell line HEK293, and undifferentiated human neuroblastoma cell line SHSY5Y were cultured in complete Dulbecco's Modified Eagle's Medium (DMEM, Gibco), which was supplemented with 10% (v/v) heat-inactivated fetal bovine serum (FBS, Gibco), 100 units/mL penicillin/streptomycin, and 1% non-essential amino acids. The cells were maintained in a humidified incubator at 37°C with an atmosphere of 5% CO_2 and 95% air, using 25 cm^2 sterile tissue culture flasks. For the MTT assay, cells were seeded into 96-well plates, while for other experimental analyses, cells were seeded into 60 mm culture dishes. Following an initial incubation period of 16–20 hours, the cells were treated with or without various concentrations of LD or LDME. Post-treatment, cells were incubated under the same conditions, and subsequent analyses were performed. All experiments were conducted in triplicate and were repeated at least three independent times to ensure reproducibility and accuracy.

Cell Viability with MTT Assay

HEK293 healthy human fibroblast cells, PLC/PRF/5 and HUH7 hepatocellular carcinoma cells, and SHSY5Y undifferentiated human neuroblastoma cells were each seeded at a density of 8,000 cells per well in 96-well culture microplates and incubated overnight at 37°C. Following the initial incubation, cells were treated for 24, 48, and 72 hours with 200 µl of fresh medium containing varying concentrations of LD and LDME (10 µM, 20 µM, 50 µM, 100 µM, and 200 µM). After the incubation periods, the medium was removed, and 100 µl of fresh medium containing 10 µl of MTT reagent (5 mg/ml) was added to each well. The cells were then incubated for an additional 2-4 hours at 37°C. Following this, the MTT-containing medium was aspirated, and 100 µl of DMSO was added to each well to dissolve the formazan crystals. The plates were then incubated for 10-20 minutes at room temperature with shaking. Absorbance was measured at 590 nm using a Varioskan Flash Multiplex Reader UV Spectrophotometer (Thermo Fisher Scientific, Waltham, MA, USA). The absorbance values were used to calculate the percentage of cell viability for each cell type. The IC_{50} values, representing the concentration required to reduce cell viability by 50% relative to DMSO-treated control cells, were calculated using GraphPad Prism 5 software and analyzed using Two-way ANOVA.

Cell Viability with Trypan Blue Staining

Dead and viable cell numbers were determined with trypan blue staining. An aliquot of cell suspension in phosphate buffered saline (PBS) was mixed with an equ-

al volume of trypan blue solution (0.4% in PBS) and cells were counted on a hemocytometer under the microscope. Trypan blue is an impermeable dye, and only dead cells with impaired membrane semi-permeability were stained with trypan blue. It is expressed as the percentage of trypan blue dead cells in the total cell population by repeated counts [21]. The viable cell percentage was calculated with the formula (Eq.1).

$$Viability\ Percentage = \frac{Live\ Cells\,(unstained)}{Total\ of\ counted\ cells\,(stained + unstained)} \times 100$$

(Eq.1)

Western Blotting

SHSY5Y cells incubated for 24 hours with the IC_{50} values of LD and LDME substances of 108.5 µM and 110.5 µM, respectively, were collected into SHSY5Y cells and lysis was performed with SDS lysis buffer containing protease/phosphatase inhibitor cocktail. Total protein concentrations were measured using the BCA Protein Assay Kit in a Vario-Scan plate reader. 50 µg of protein was separated by 10% SDS-PAGE, then transferred to nitrocellulose membrane. After blocking non-specific bindings with 5% skim milk powder in TBS + 1% Tween-20, the membranes were incubated with primary antibodies O/N at 4 ˚C.

For apoptosis analysis; as primer antibodies PARP, Cleaved Caspase 3, p53, and as secondary antibodies anti rabbit (Advansta) and anti-mouse (Advansta) were used. The GAPDH (CST) antibody used as a loading control was used. Proteins were detected using an ECL reagent (Advansta) and analyzed with the Chemi Doc XRS+ System (Bio-Rad, Hercules, CA, USA).

Apoptosis

SHSY5Y cells were seeded at 60% density in a 60 mm cell dish, the next day LD and LDME substances of 108.5 µM and 110.5 µM, respectively, were added and incubated for 24 hours. After incubation, cells were harvested and the cell pellet was washed with cold PBS, resuspended in 1X binding buffer. FITC-labeled Annexin V (5 µl) and PI (5 µl) were added to SHSY5Y cells, followed by incubation for 15 minutes at room temperature and in the dark. Cell apoptosis was assessed by flow cytometry (BD-Accuri, BD Bioscience, Franklin Lakes, NJ, USA).

Cell Cycle

SHSY5Y cell line was seeded at 60% density in 60 mm cell dishes. The next day, medium containing LD and LDME substances of 108.5 µM and 110.5 µM, respectively, were was added to the appropriate cell dishes and incubated for 24 hours, after which the cells were washed with PBS (ice-cold) and fixed using cold 70% ethanol. After washing again with PBS, the cells were incubated for 1 hour at 37 °C in the dark in dye solution (PBS containing 0.1% Triton X-100, 1 mg/ml RNase A and PI (50 µg/ml, Bio-Legend). Depending on the abundance of the PI-DNA complexes in the cell, the amount of emitted fluorescent light was measured by flow cytometry (BD-Accuri, BD Bioscience, Franklin Lakes, NJ, USA) and the cell density at different stages of the cell cycle was determined as a percentage.

Statistics and Data Analysis

Each experiment was performed at least three times, and representative data are shown. Data in bar graphs are given as the means ± S.D. Means were checked for the statistical difference using the t-test and p-values less than 0.05 were considered significant (*p <0.05, **p <0.01, ***p <0.001). The IC_{50} value was calculated using GraphPad. The IC_{50} was defined as the concentration that gave rise to a 50% viable cell number.

Computational Details

The optimized structures of the LD and LDME compounds were determined using the Gaussian 09W package [22] and Gauss View 5.0 interface [23] tools, respectively, using the DFT/B3LYP theory/functional and 6-311++G(d,p) basis set. The calculations were carried out in the Gas phase. Using AutoDock Vina [24] the ensuing in silico molecular docking calculations were carried out.

RESULTS and DISCUSSION

Determination of the MIC Value

Table 1 presents the minimal inhibitory concentrations of LD and LDME. All two compounds were found to have no effect on the growth of Gram-negative bacteria at any concentration. However, LD and LDME inhibited Gram-positive bacteria. The MIC values for them were 250 and 1000 µM, respectively (Table 1).

Table 1. MIC values of the L-DOPA and L-DOPA methyl ester.

	MIC [µM/L]	
	E. coli	*S. aureus*
L-DOPA	-	250
L-DOPA methyl ester	-	1000
Ampicillin	7.8	<3.9
Streptomycin	<3.9	<7.8

The LD and LDME compounds were shown to have an antibacterial impact on Gram-positive bacteria but no effect on Gram-negative bacteria when their antimicrobial characteristics were investigated. Similar findings have been found in the literature. In one study, PEGylated dopamine ester (PDE) was synthesized, and its antimicrobial properties were investigated against Gram-negative bacteria, Gram-positive bacteria. The compound has been shown to be effective against all tested strains [25]. In another study, when the antimicrobial properties of synthesized DOPA esters were examined, it was observed that they showed the highest antimicrobial effect against Gram-positive *S. aureus* with an MIC value of 249 mM [18]. It is possible that this is because of the presence of a membrane on the exterior of the *E. coli* cell wall or that the process of inactivation of the organism differs [26]. This cell membrane may be more resistant to LD and LDME substances and may enable bacteria to survive and flourish in conditions that are lethal to *S. aureus*. Contrarily, LD and LDME substances may interact with the *S. aureus* cell membrane, increasing its permeability and perhaps causing depolarization, lysis, and cell death [8]. Similar to this, it's possible that the LD and LDME compounds' inability to interact with E. coli was due to the differences in cell wall composition between Gram-positive and Gram-negative bacteria [26,27]. The study's findings demonstrated that LD and LDME compounds were effective at killing Gram-positive bacteria. Therefore, it is very likely that new antimicrobial compounds with enhanced antibacterial activity and a broad spectrum would be produced by synthesizing different L-DOPA compounds. Research on different drug classes shows that tricyclic phenothiazines have antimicrobial properties. Studies on literature showed that aromatic rings are the source of antimicrobial properties of some agents [28].

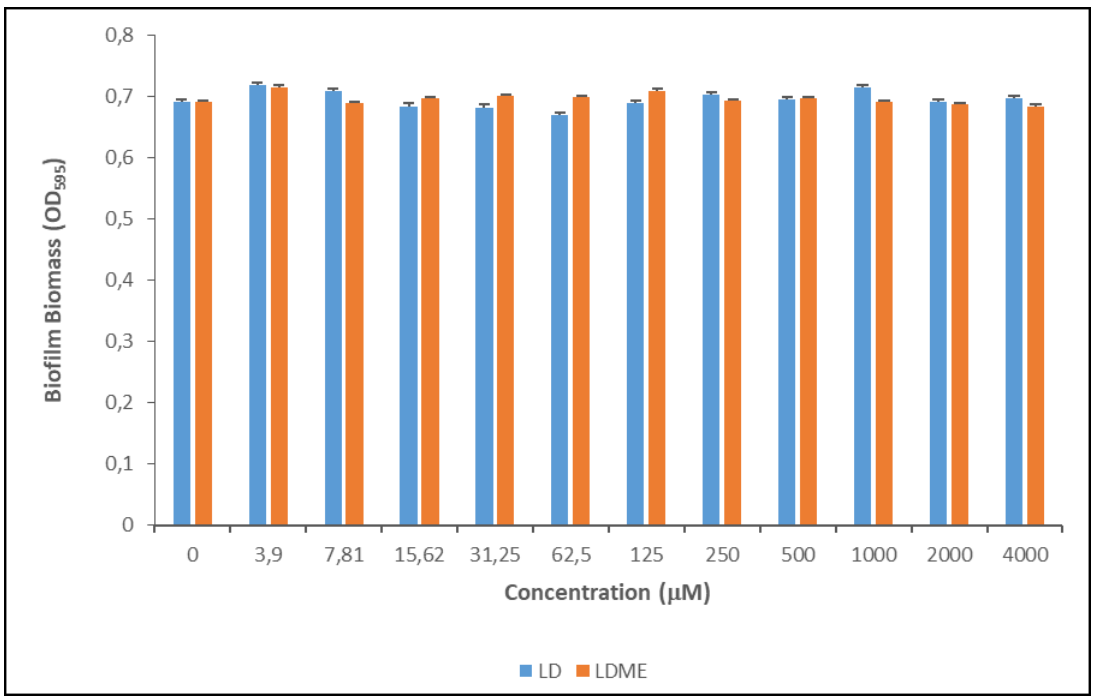

Figure 1a. Antibiofilm activity of the indicated LD and LDME concentrations (3.9 to 4000 µM) on *E. coli* after 96 hours of incubation.

Antibiofilm Activity

We tested the antibiofilm properties of LD and LDME compounds with concentrations ranging from 3.9 to 4000 mM using a modified static biofilm assay [29]. Even at the highest LD and LDME concentrations used, none of the compounds prevented *E. coli* from forming biofilms (Figure 1a). *S. aureus* biofilm formation was dose-dependently reduced for LD and LDME, resulting in approximately 53% and 49% reductions in biofilm biomass at the highest concentration tested (4000 mM), respectively (Figure 1b).

LD and LDME Induced a Reduction in the Viability of Cancer Cells in a Concentration-Dependent and Time-Dependent Manner.

To evaluate the effect of LD and LDME on cell viability, HEK293, PLC/PRF/5, HUH7 and SHSY5Y cell lines were exposed to increasing concentrations (0-500 µM) over 72-hour period, with cell viability assessed using the MTT method. In the PLC/PRF/5 cell line, both LD and LDME reduced cell viability in a dose- and time-dependent manner, with LD demonstrating greater efficacy at lower concentrations compared to LDME (Fig. 2a). Similarly, in the HUH7 cell line, LD significantly decreased cell viability in a dose- and time-dependent manner, whereas LDME only partially reduced viability, with cell viability remaining above 70% at all tested doses, thus precluding the calculation of an IC_{50} value (Figure 2a). In the SHSY5Y cell line, both LD and LDME notably decreased cell viability, particularly at lower doses, when compared to other cancer cell lines (Fig. 2a). Across all three cancer cell lines, LD consistently exhibited greater potency in reducing cell viability than LDME. Additionally, at higher doses, both LD and LDME were effective in reducing cell viability in the non-cancerous HEK293 cell line (Fig. 2a). Inhibition graphs are detailed in Fig. 3, as LD and LDME substance administrations in SHSY5Y cells cause a dose- and time-dependent change on cell viability (Figure 2b).

IC_{50} values calculated with the GraphPad program were calculated for all cell lines. The IC_{50} values also quantitatively indicate that the anti-proliferative property of LD is more effective than LDME (Table 2). However, when the cell viability results are examined, it is a pleasing and promising result that the IC_{50} values calculated for the SHSY5Y cell are not toxic to the healthy cell line HEK293.

LD and LDME Induce Cytotoxicity in Human Cancer Cells with Tryphan Blue Assay

When HEK293, PLC/PRF/5, HUH7, and SHSY5Y cell lines were exposed to LD and LDME, time and dose-dependent decreasing cell viability was recorded by trypan

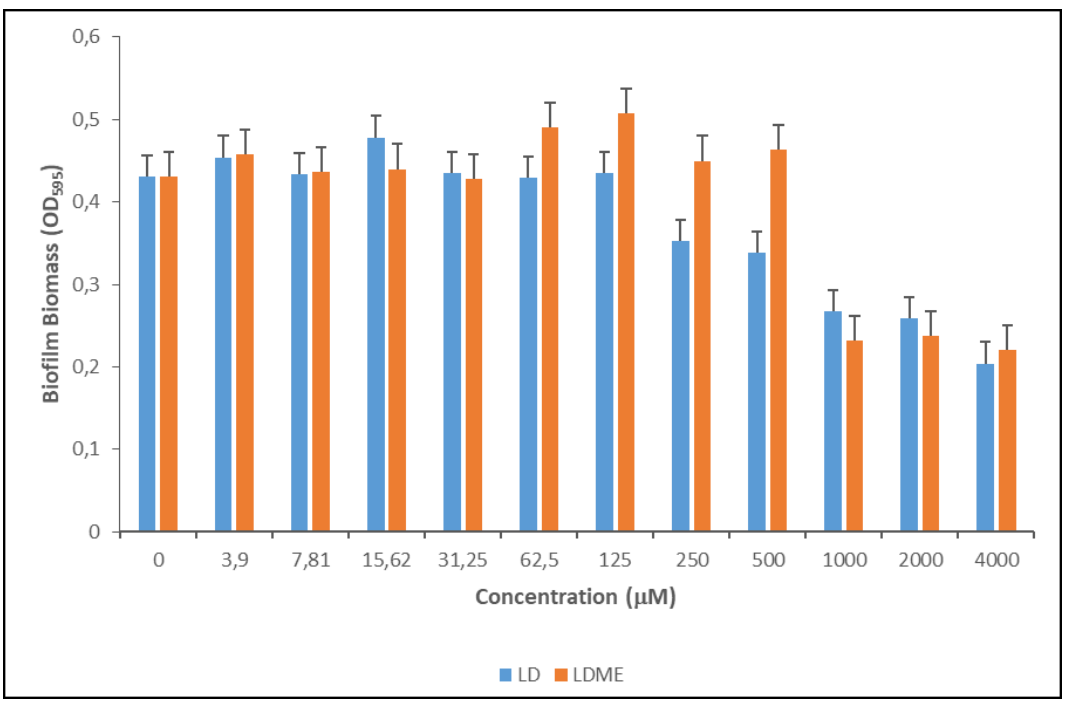

Figure 1b. Antibiofilm activity of the indicated LD and LDME concentrations (3.9 to 4000 µM) on S. aureus after 96 hours of incubation.

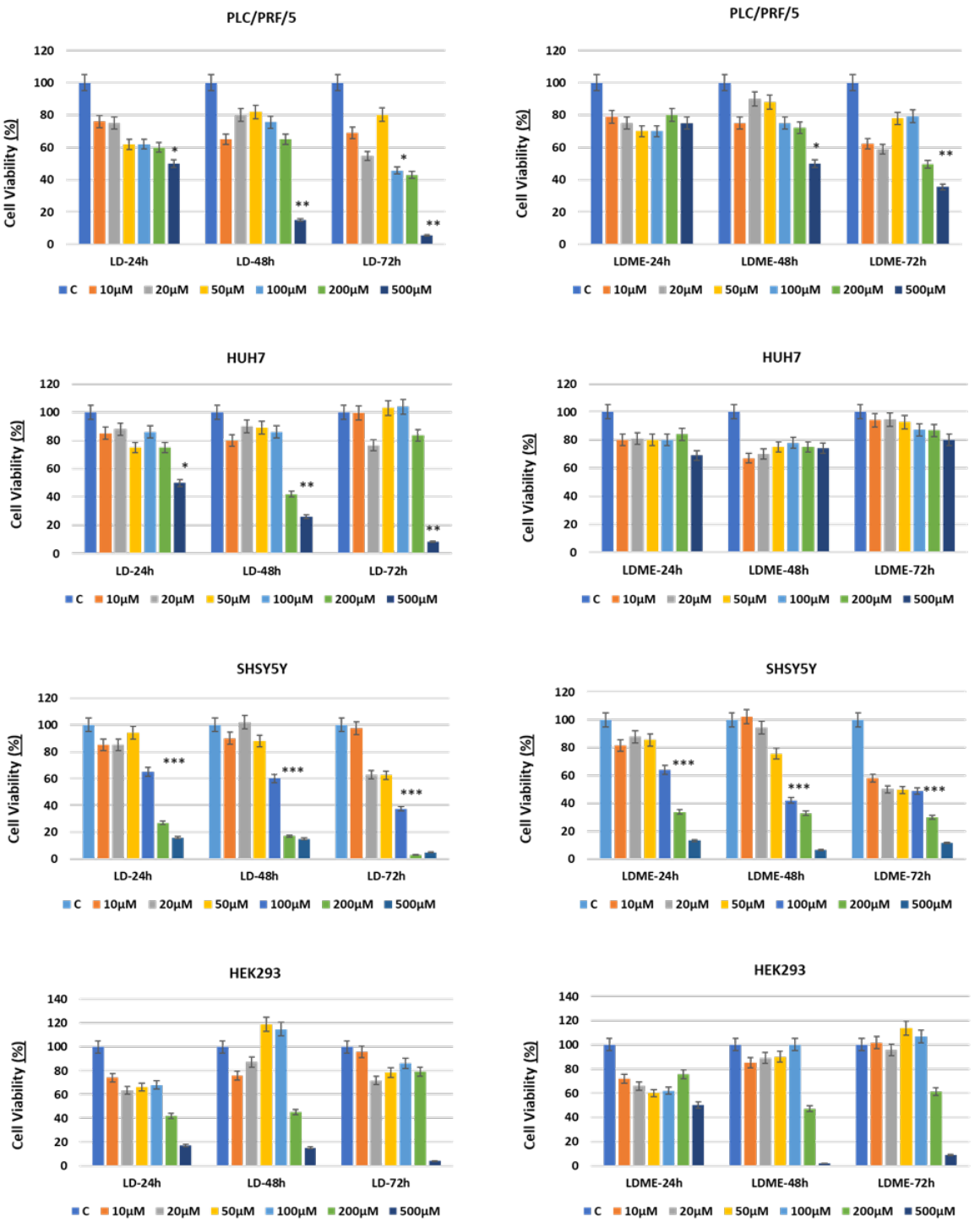

Figure 2a. Viability effects of LD and LDME on the human cell lines. Cells were incubated for 24h, 48h, 72h with a range of LD and LDME concentrations and their viability was measured by MTT assay data showing the optical density (OD). Cell viability was expressed as relative cell viability compared to control, and the data shown are the most representative of 3 separate experiments. (*p <0.05, **p <0.01, ***p <0.001).

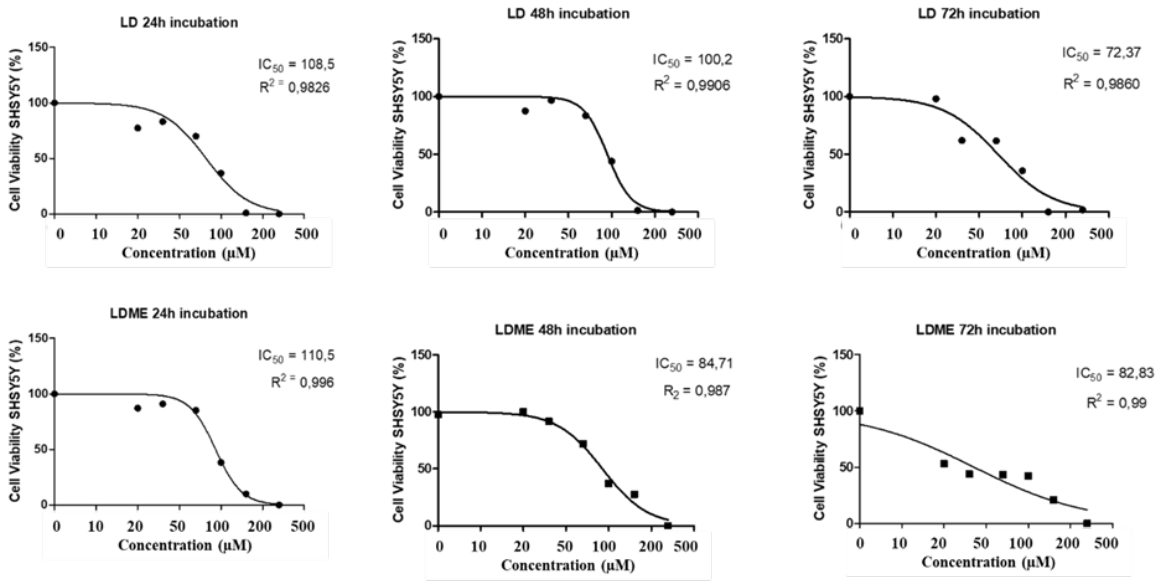

Figure 2b. Viability effects of LD and LDME on the human cell lines. The graphs show the 50% inhibitory concentrations (IC_{50}) of the LD and LDME in SHSY5Y cell line at 24, 48 and 72 h.

staining (Figure 3). The results obtained with trypan staining show parallelism with the cell viability results obtained with the MTT assay.

LD and LDME Treatment Induce Increased Apoptotic Pathway Related Proteins

Twenty-four hours after treatment of the SHSY5Y cell line with LD and LDME at their respective IC_{50} concentrations, the cells' resistance to apoptosis was assessed by evaluating the cleavage of the PARP protein (p89 PARP), a marker of apoptosis induction [30,31]. Western blot analysis revealed an increased PARP cleavage fraction in both LD- and LDME-treated cells compared to the control group. Specifically, PARP expression increased 1.3-fold following LD treatment and 2.9-fold following LDME treatment relative to the control (Figure 4a). Additionally, the expression of another key apoptotic marker, caspase-3, was analyzed [32]. A notable increase in caspase-3 expression was observed in both treatment groups compared to the control. LD treatment resulted in a 1.9-fold increase in caspase-3 expression, while LDME treatment led to a 1.2-fold increase (Figure 4a). Interestingly, the expression of p53, another well-established apoptotic marker, showed differential regulation following treatment: p53 expression increased by 0.8-fold after LD treatment and by 1.2-fold following LDME treatment (Figure 4a). These changes in protein expression were normalized to GAPDH to account for any variations in loading controls, and quantitative analysis was performed to compare the protein levels between the LD and LDME treatment groups and the control group. Furthermore, to determine the cells' susceptibility to apoptosis, Annexin V/7-AAD staining was conducted and analyzed using BD Accuri C6 flow cytometry. This assay provided additional insights into whether the cells exhibited resistance to the apoptotic response following LD and LDME treatments.

LD and LDME Treatment Induce Apoptosis

To determine whether LD and LDME cause cell death by apoptosis, AnnexinV/7AAD staining with LD and LDME on the SHSY5Y cell line was performed and analyzed by BD Accuri C6 FACS. As shown in Fig.4b, when SHSY5Y cells were treated with IC 50 values of 108.5uM and 110.5uM for 24 hours, it was shown that LD application led to apoptosis in 78.8% and LDME application in 68.5% (Figure 4b).

LD and LDME Treatment Cause of Cell Cycle Arrest at Differents Levels

Cell cycle analysis by flow cytometry was performed to explain the altered proliferation status of LD and LDME administration in the SHSY5Y cell line. Cells stained with PI (propidium iodide) dye were analyzed by BD Accuri C6 FACS. It has been shown that LD application causes aggregation of cells, especially in the G2/M phase. However, in LDME application, cells are halted in the G1 and S phases and far fewer cells can progress to the G2/M phase (Figure 5).

Table 2. IC_{50} values.

	HEK293		PLC		HUH7		SHSY5Y	
IC_{50} (µM)	LD	LDME	LD	LDME	LD	LDME	LD	LDME
24h	212.78	220.4	500	-	500	-	108.5	110.5
48h	254.9	259.6	227.9	500	170	-	100.2	84.71
72h	252.83	202.2	97.63	270.5	375.2	-	72.37	82.83

Molecular Docking Analysis

By simulating the interaction between a small molecule and a protein at the atomic level, the molecular docking method enables us to characterize how small molecules behave at the binding site of target proteins and to better understand fundamental biological processes [33,34]. Therefore, based on both temporal and financial outcomes, we can state that this methodology is a crucial foundation for the development of novel drugs. Although there are many in-silico models, we found that Autodock Vina 24 [5], an open source and cost-free computational tool for molecular docking, was more efficient for our calculations. In this part, PDB: 2DS2 [35], PDB: 4URO [36] and PDB: 1M17 [37] proteins were determined as antimicrobial, antibacterial and anticancer targets for LD and LDME molecules.Molecular optimization for LD and LDME was done before docking by using DFT/B3LYP theory/functional and 6-311++G(d,p) basis set within the Gaussian 09W [22], and then output file was recorded as PDB (protein data bank) format. Here, numbering formats for the ligands (LD and LDME) were derived from the output and the resulting structures were shown as in Figure 6.

The sum of electronic and zero-point energies for LD and LDME compounds were computed as -705.45876096 a.u. and -1205.59852691 a.u., respectively. In other words, according to the results, we can say that the LDME molecule is more stable than the LD molecule. The 3D structure of the used three proteins (PDBs: 2DS2, 4URO and 1M17) as targets in the docking calculation was obtained from the Protein Data Bank-RCSB [38]. Afterwards, the co-factors and the water molecules in the proteins were deleted and polar hydrogen charges were added and then the proteins were saved as PDB format. The Discover Studio Visualizer 4.0 (DSV 4.0) program [39] was used to create the PDB structures of both ligands and proteins and to make the necessary

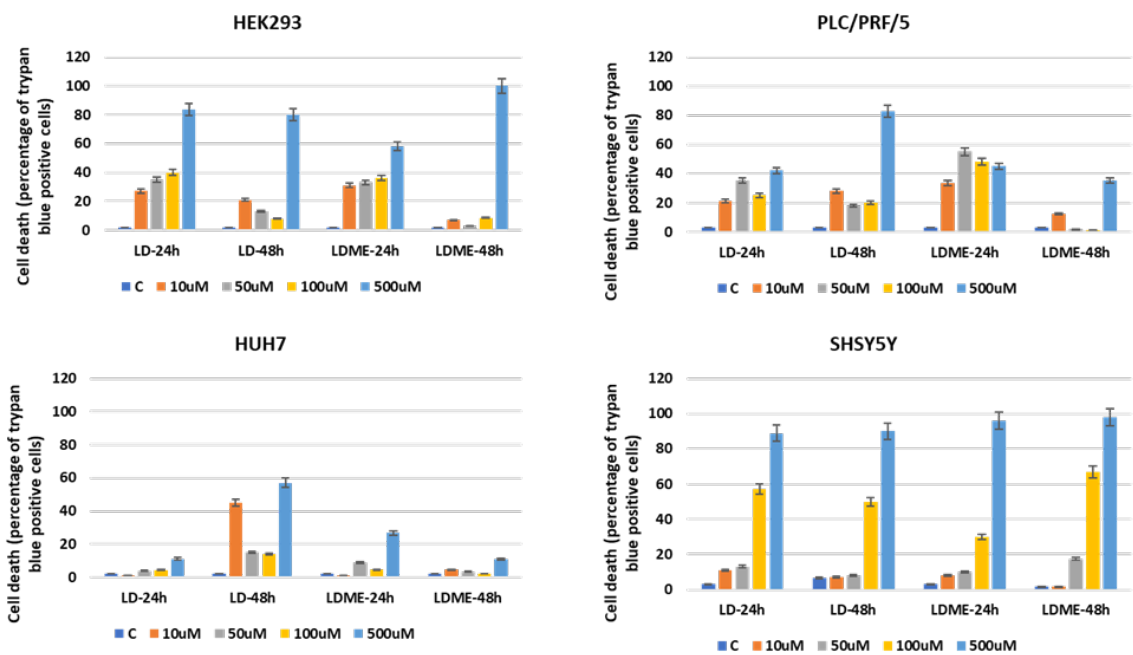

Figure 3. Dose-dependent effects of LD and LDME on the cell-viability of the human cell lines. Cells were treated without (control) or with varying concentrations of LD or LDME (10-500 µM) for 24 h and 48h and the cell viability was measured by trypan blue assay. Values are the means ± SD of six observations.

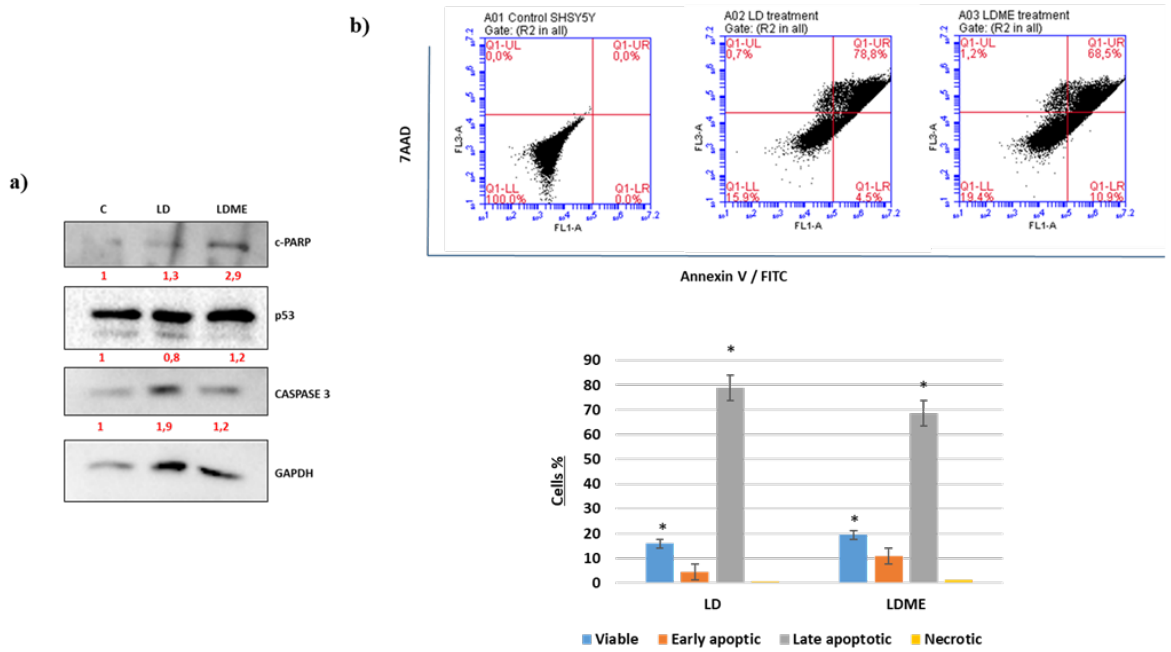

Figure 4a. Alteration levels of apoptotic proteins after treatment with LD and LDME in SHSY5Y cell line.

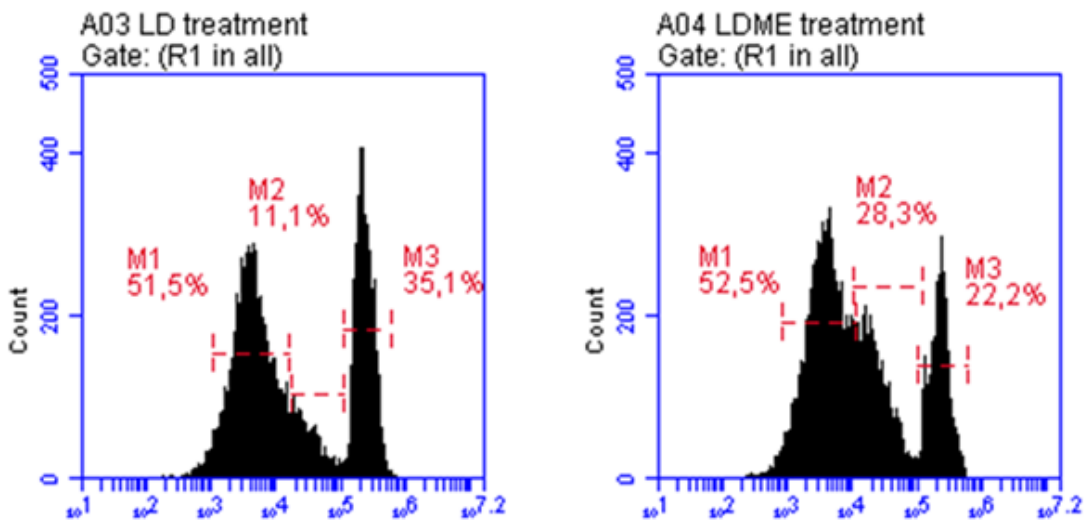

Figure 5. Effect of LD and LDME on SHSY5Y cell cycle profile. SHSY5Y cells were exposed to 108.5 and 110.5 µM concentrations of LD and LDME, respectively. Cell cycle analysis of shPLXNC1 and PLKO cell clones M1 G1, M2 S and M3 indicate the G2/M phases.

preparations. Now let's examine the interactions that exist between the chosen targets and ligands, correspondingly.

For antimicrobial target (PDB: 2DS2 [35]), firstly the active sites for C+D chains were determined as ARG70, PHE69, PHE49, ARG27, ARG24, since there are no active residues in the A and B chains. Considering these residues, the necessary grid parameters for the molecular docking calculation were as follows:40x82x40Å^3 x, y, z dimensions, 0.375 Å space, and 16.734, 4.887, 1.706 x,y,z centers. Taking these dimensions, the obtained binding energies in the interactions between LD+2DS2 and LDME+2DS2 were found to be -5.6 kcal/mol and -5.1 kcal/mol, respectively. Using these binding energy values and Ki=exp(ΔG/RT) equation (G-binding energy, R-gas constant=1.987203610^{-3} kcal/mol, and T- room temperature=298.15K), inhibition constants were found to be 78.5543µM and 182.672 µM, respectively. These scores were tabulated in Table 3. Since the binding energy of the LD molecule to the related protein (PDB: 2DS2) is higher, the 3D (a) and 2D (b) forms of this interaction and the insertion of the ligand into the protein (c) can be given as in Figure7.

As seen from Figure7 (b), two conventional hydrogen bonding between ARG14 and O1 with 3.07 Å and between GLN32and O1 with 3.04 Å were observed. Additionally, π-alkyl interaction between ARG16 and the center of benzene with 5.00 Å were seen. For LDME+PDB: 2DS2 molecular docking results were indicated as in Figure S1 (Supporting Information).

Second, if we look at the results for the antibacterial target (PDB: 4URO) 36 [19], the active sites for A chain were determined as ARG144, SER128, ILE102, GLN91, ASP89, PRO87, ILE86, GLY85, ARG84, ASP81, GLU58, ASP57, SER55, ASN54. Considering these active residues, the necessary grid parameters for the molecular docking calculation were as follows:62x48x78 Å^3 x, y, z dimensions, 0.375 Å space, and -2.597, -2.639, -12.676 x, y, z centers. Taking these dimensions, the obtained binding energies in the interactions between LD+4URO and LDME+4URO were found to be -7.2 kcal/mol and -6.3 kcal/mol, respectively. Using these binding energy values and the above equation, inhibition constants were found to be 5.27669 µM and 24.1027 µM, respectively. These scores were presented in Table 3. Since the binding energy of the LD molecule to the related protein (PDB: 4URO) is higher, the 3D (d) and 2D (e) forms of this interaction and the insertion of the ligand into the protein (f) can be given as in Figure 7. As seen from Figure 7 (e), five conventional hydrogen bondings between ARG84and O3 with 3.32 Å, between THR173 and O1 with 2.99 Å, between GLU58 and H17 with 2.11 Å, between SER128 and H22 with 2.78 Å and between SER128 and H23 with 2.20 Å were observed. Additionally, π-sigma interaction between ILE86 and the center of benzene with 3.64 Å were seen. For LDME+PDB: 4URO molecular docking results were indicated as in Figure. S2 (Supporting Information).

Thirdly, if we look at the results for the anticancer target (PDB: 1M17) 37[20], the active sites for A chain

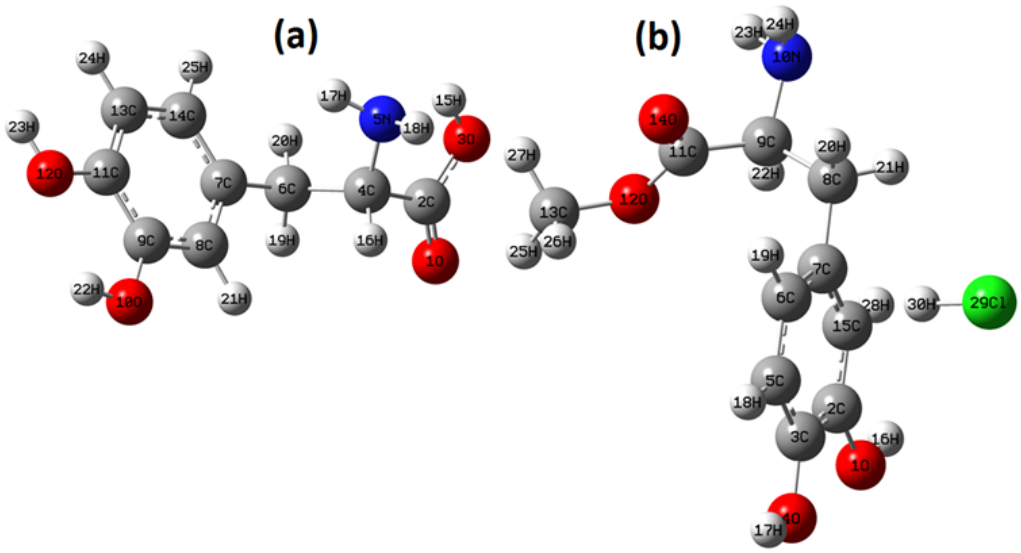

Figure 6. The optimized structures of LD and LDME molecules.

Table 3. Molecular docking scores of L-DOPA and L-DOPA methyl ester molecules.

Antimicrobial target/PDB: 2DS2			
Compound	Binding Energy (kcal/mol)	The number of hydrogen bonding	Ki (μM)
L-DOPA	-5.6	2	78.5543
L-DOPA methyl ester	-5.1	1	182.672
Antibacterial target/PDB: 4URO			
Compound	Binding Energy (kcal/mol)	The number of hydrogen bonding	Ki (μM)
L-DOPA	-7.2	5	5.27669
L-DOPA methyl ester	-6.3	1	24.1027
Anticancer target/PDB: 1M17			
Compound	Binding Energy (kcal/mol)	The number of hydrogen bonding	Ki (μM)
L-DOPA	-8.7	7	0.419618
L-DOPA methyl ester	-6.4	4	20.3594

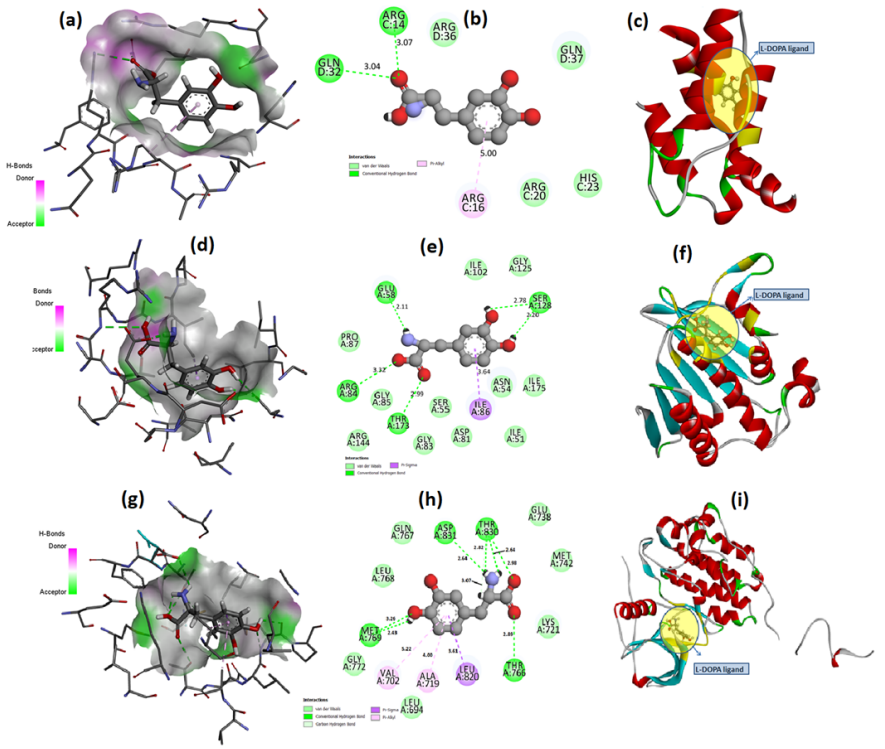

Figure 7. The 3D (a, d, g), 2D (b, e, h) forms of the LD+2DS2 and the insertion of the LD into the proteins (c, f, i).

were determined as ASP831, THR830, LEU820, GLY772, PHE771, PRO770, MET769, LEU768, GLN767, THR766, LEU764, ALA719, LEU694. Considering these active residues, the necessary grid parameters for the molecular docking calculation were as follows: 64x58x60 $Å^3$ x, y, z dimensions, 0.375 Å space, and 23.256, -2.289, 56.367 x, y, z centers. Taking these dimensions, the obtained binding energies in the interactions between LD+1M17 and LDME+1M17 were found to be -8.7 kcal/mol and -6.4 kcal/mol, respectively. Similarly, using these binding energy values and the above equation, inhibition constants were found to be 0.419618 μM and 20.3594 μM, respectively. These scores were given in Table 3. Since the binding energy of the LD molecule to the related protein (PDB: 4URO) is higher, the 3D (g) and 2D (h) forms of this interaction and the insertion of the ligand into the protein (i) can be given as in Figure 7. As seen from Figure 7 (h), seven conventional hydrogen bonding between MET769and O13 with 3.26 Å, between MET769 and O13 with 2.43 Å, between THR766 and O1 with 2.89 Å, between ASP831and H17 with 2.64 Å, between THR830 and H17 with 2.82 Å, between THR830

and H18 with 2.64 Å and between THR830 and O3 with 2.89 Å. Additionally, π-sigma interaction between LEU820 and the center of benzene with 3.61 Å, π-alkyl interactions between VAL702 and the center of benzene with 5.22 Å and between ALA719 and the center of benzene with 4.00 Å were detected. For LDME+PDB: 1M17 molecular docking results were indicated as in Figure S3 (Supporting Information).

If the obtained in-silico molecular docking results so far are summed up, we can state that the LD molecule can be considered as more potential for antimicrobial, antibacterial and anticancer targets. We can say that it is a good drug candidate, especially considering the hydrogen bonds it captures and binds to the LD molecule anticancer/PDB: 1M17 target with its high bound energy.

CONCLUSION

In our research, we evaluated the antibacterial effects of L-DOPA and L-DOPA methyl ester compounds on gram-positive and gram-negative bacteria. Both compounds demonstrated antibacterial activity against gram-positive bacteria, with LD showing a greater inhibitory effect on the growth of gram-positive bacteria compared to LDME. Also, our study further revealed that both LD and LDME exhibit anti-cancer activity by reducing cell viability, primarily through the induction of apoptosis and modulation of the cell cycle. These effects were particularly pronounced in cancer cells of brain origin, suggesting that LD may be a promising candidate for the treatment of brain-related cancers. The data support the potential for further in vivo studies to explore the therapeutic efficacy of LD based on these findings. Additionally, molecular docking interactions between the three target proteins and LD/LDME ligands were performed with Autodock Vina. The results indicated that the LD molecule demonstrated superior docking affinity to the target receptors compared to the LDME molecule, correlating with stronger inhibitory effects. These findings not only enhance our understanding of the drug potential of the molecules under study but also underscore the value of integrating both theoretical and experimental approaches. The insights gained from this research are expected to guide and inform future studies aimed at developing improved therapeutic strategies in this field.

Acknowledgement
The authors especially thanks to Prof. Dr. Fatih UCUN for his helpful contribution for Gaussian calculations.

References

1. S.T. Cole, Who will develop new antibacterial agents? Philos. Trans. R. Soc. Lond. B. Biol. Sci., 369 (1645) (2014) 20130430.
2. A. Pinazo, R. Pons, L. Perez, M.R. Infante, Amino acids as raw material for biocompatible surfactants, Ind. Eng. Chem. Res., 50 (9) (2011) 4805–4817.
3. M. Markovic, S. Ben-Shabat, A. Dahan Prodrugs for Improved Drug Delivery: Lessons Learned from Recently Developed and Marketed Products Pharmaceutics, 12 (11) (2020) 1031-1043.
4. X. Sun, S.Vilar, N.P. Tatonetti, High-throughput methods for combinatorial drug discovery. Sci. Transl. Med., 5 (2013) 201-205.
5. D. Gupta, D. Bhatia, V. Dave, V. Sutariya, Varghese Gupta, S., Salts of Therapeutic Agents: Chemical, Physicochemical, and Biological Considerations, Molecules, 23 (2018) 1719.
6. V.J.Stella, K.W. Nti-Addae, Prodrug strategies to overcome poor water solubility, Adv. Drug Deliv. Rev., 59 (2007) 677–694.
7. Y. T. H. Lam, M.G. Ricardo, R.Rennert, A. Frolov, A.Porzel, W. Brandt, P. Stark, B. Westermann, N. Arnold, Rare glutamic acid methyl ester peptaibols from Sepedonium ampullosporum damon KSH 534 exhibit promising antifungal and anticancer activity. Int. J. Mo.l Sci., 22 (23) (2021) 12718.
8. N. Joondan, S. Jhaumeer-Laulloo, P. Caumul, A study of the antibacterial activity of L-phenylalanine and L-tyrosine esters in relation to their CMC and their interactions with 1,2-dipalmitoylsn- glycero-3-phosphocholine, DPPC as model membrane. Microbiol. Res., 169 (2014) 675–685.
9. N. Joondan, P. Caumul, M. Akerman, S. Jhaumeer-Laulloo, Synthesis, micellization and interaction of novel quaternary ammonium compounds derived from L-phenylalanine with 1,2-dipalmitoyl-sn-glycero-3-phosphocholine as model membrane in relation to their antibacterial activity, and their selectivity over human red blood cells, Bioorg. Chem., 58 (2015) 117–129.
10. A. Bratuša, T. Elschner, T. Heinze, E. Fröhlich, S.Hribernik, M.Božič, E. Žagar, K.S. Kleinschek, M.Thonhofer, R. Kargl, Functional dextran amino acid ester particles derived from N-protected S-trityl-L-cysteine, Colloids Surf. B., 1:181 (2019) 561-566.
11. J.A.S. Almeida, M.C. Moran, M.R. Infante, A.A.C.C. Pais, Interaction of arginine-based cationic surfactants with lipid membrane. An experimental and molecular simulation study, Arkivoc, 34 (2010) 34–40.
12. N. Lozano, L. Perez, R. Pons, J.R. Luque-Ortega, M. Fernandez-Reyes, L. Rivas, A. Pinazo, Interaction studies of diacyl glycerol arginine-based surfactants with DPPC and DMPC monolayers, relation with antimicrobial activity, Colloids Surf. A., 319 (2008) 196-203.
13. S. Fahn MD, Levodopa in the treatment of Parkinson's disease, Oxidative Stress and Neuroprotection J. Neural Transm. Suppl., 71 (2006) 1-15.
14. R. Hernández-Altamirano, V. Y. Mena-Cervantes, T.E. Chávez-Miyauchi, D.A. Nieto-Álvarez, M. A. Domínguez-Aguilar, L. S. Zamudio-Rivera,V. Barba, F.J. Fernández-Perrino, S. Pérez-Miranda f, H. I. Beltrán, New bis-di-organotin compounds derived from aminoacid-imine-hexadentate ligands, Multifunctional evaluation as corrosion inhibitors, antibacterials and asphaltene dispersants/inhibitors, Polyhedron, 52 (22) (2013) 301-307.

15. D.R. Cooper, C.Marrel, B. Testa, H. Van de Waterbeemd, N. Quinn, P. Jenner, C.D., Marsden, L-Dopa methyl ester--a candidate for chronic systemic delivery of L-Dopa in Parkinson's disease, Clin. Neuropharmacol., 7(1) (1984) 89-98.
16. D.R.Cooper, C. Marrel, H. Van de Waterbeemd, B. Testa, P.Jenner, C.D.Marsden, L-dopa esters as potential prodrugs: effect on brain concentration of dopamine metabolites in reserpinized mice, J. Pharm. Pharmacol., 39 (10) (1987) 809-18.
17. N.Furukawa, Y. Goshima, T. Miyamae, Y.Sugiyama, M. Shimizu, E. Ohshima, F. Suzuki, N. Arai, K. Fujita, Y. Misu, L-DOPA Cyclohexyl ester is a novel potent and relatively stable competitive antagonist against L-DOPA among several L-DOPA ester compounds, Jpn. J. Pharmacol., 82 (2000) 40-47.
18. N. Joondan, S. Jhaumeer-Laulloo, P. Caumul, Effect of Chain Length on the micellization, antibacterial, DPPC interaction and antioxidant activities of L-3,4- Dihydroxyphenylalanine (L-DOPA) esters, J. Surfact. Deterg., (2015) 18:1095–1104.
19. M.M. Wick, L-Dopa methyl ester as a new antitumour agent, Nat., 269 (1977).
20. M. Balouiri, M. Sadiki, S.K. Ibnsouda, Methods for in vitro evaluating antimicrobial activity: A review, J. Pharm. Anal., 6 (2) (2016) 71-79.
21. O. Yermolaieva, R. Xu, C. Schinstock, N. Brot, H. WEissbach, S.H. Heinemann, T. Hoshi, Methionine sulfoxide reductase A protects neuronal cells against brief hypoxia/reoxygenation, Proc. Natl. Acad. Sci. U.S.A., 101 (5) (2004) 1159-1164.
22. M.J. Frisch, G. Trucks, H. Schlegel, G. Scuseria, M. Robb, J. Cheeseman, G. Scalmani, V. Barone, B. Mennucci, G. Petersson, Gaussian 09, Revision D. 01, Gaussian, Inc. Wallingford, CT (2009).
23. R. Dennington, T. Keith, J. Millam, GaussView, version 5, Semichem Inc.: Shawnee Mission, KS (2009).
24. O. Trott, A.J. Olson, AutoDock Vina: improving the speed and accuracy of docking with a new scoring function, efficient optimization, and multithreading, J. Comput. Chem., 31 (2) (2010) 455-461.
25. A.Thakur, S. Ranote, D. Kumar, K.K. Bhardwaj, R. Gubta, G.S. Chauhan, Synthesis of a PEGylated dopamine ester with enhanced antibacterial and antifungal activity, ACS Omega, 3 (7) (2018) 7925-7933.
26. T.J. Silhavy, D. Kahne, S. Walker, The Bacterial Cell Envelope, Cold Spring Harb. Perspect. Biol., 2 (5) (2010) 000414.
27. N. Malanovic, K. Lohner, Gram-positive bacterial cell envelopes: The impact on the activity of antimicrobial peptides, Biochim. Biophys. Acta- Biomembr., 1858 (5) (2016) 936-946.
28. M. Sushomasri, S.M. Himangshu, C. Pranabesh, G.D. Sujata, Potential of dopamine hydrochloride as a novel antimicrobial agent, Int. J. Biomed. Pharm. Sci., 4 (2) (2010) 70-75.
29. J. Lellouche, E. Kahana, S. Elias, A. Gedanken, E.Banin, Antibiofilm activity of nanosized magnesium flüoride, J. Biomater., 30 (2009) 5969-5978.
30. S.H.Kaufmann, S. Desnoyers, Y. Ottaviano, N.E. Davidson, G.G.Poirier, Specific Proteolytic Cleavage of Poly(ADP-ribose) Polymerase: An Early Marker of Chemotherapy-induced Apoptosis, Cancer Research, 53 (1993) 3976–3985.
31. M.Tewari, L.T. Quan, K. O'Rourke, S. Desnoyers, Z. Zeng, D.R. Beidler, G.G. Poirier, G.S. Salvesen, V.M. Dixit, Yama/ CPP32b, a mammalian homolog of CED-3, is a CrmA-inhibitable protease that cleaves the death substrate poly (ADP-ribose) polymerase, Cell, 81 (1995) 801–809.
32. Y. Zhang, A. Dimtchev, A. Dritschilo, M. Jung, Ionizing Radiation-induced Apoptosis in Ataxia-Telangiectasia Fibroblasts: Roles of caspase-9 and cellular inhibitor of apoptosis protein-1, J. Biol. Chem., 276 (2001) 28842–28848.
33. B.J. McConkey, V. Sobolev, M. Edelman, The performance of current methods in ligand–protein docking, Curr. Sci., 83 (7) (2002) 845-856.
34. S.F. Sousa, P.A. Fernandes, M.J. Ramos, Protein–ligand docking: current status and future challenges, Proteins: Struct., Funct., Bioinf., 65 (1) (2006) 15-26.
35. D.-F. Li, P. Jiang, D.-Y. Zhu, Y. Hu, M. Max, D.-C. Wang, Crystal structure of II: a structural type of sweet proteins and the main structural basis for its sweetness, J. Struct. Biol., 162 (1) (2008) 50-62.
36. J. Lu, S. Patel, N. Sharma, S.M. Soisson, R. Kishii, M. Takei, Y. Fukuda, K.J. Lumb, S.B. Singh, Structures of kibdelomycin bound to Staphylococcus aureus GyrB and ParE showed a novel U-shaped binding mode, ACS Chem. Biol., 9 (9) (2014) 2023-2031.
37. J. Stamos, M.X. Sliwkowski, C. Eigenbrot, Structure of the epidermal growth factor receptor kinase domain alone and in complex with a 4-anilinoquinazoline inhibitor, J. Biol. Chem., 277 (48) (2002) 46265-46272.
38. S.F Sousa, P.A Fernandes, M.J Ramos, Protein–ligand docking: current status and future challenges, Proteins: Struct., Funct., Bioinf., 65 (1) (2006) 15-26.
39. T.Kimmerlin, Discovery and optimization of isoquinoline ethyl ureas as antibacterial agents, J. Med. Chem., 60 (9) (2017) 3755-3775.

Figure captions of Supporting Information

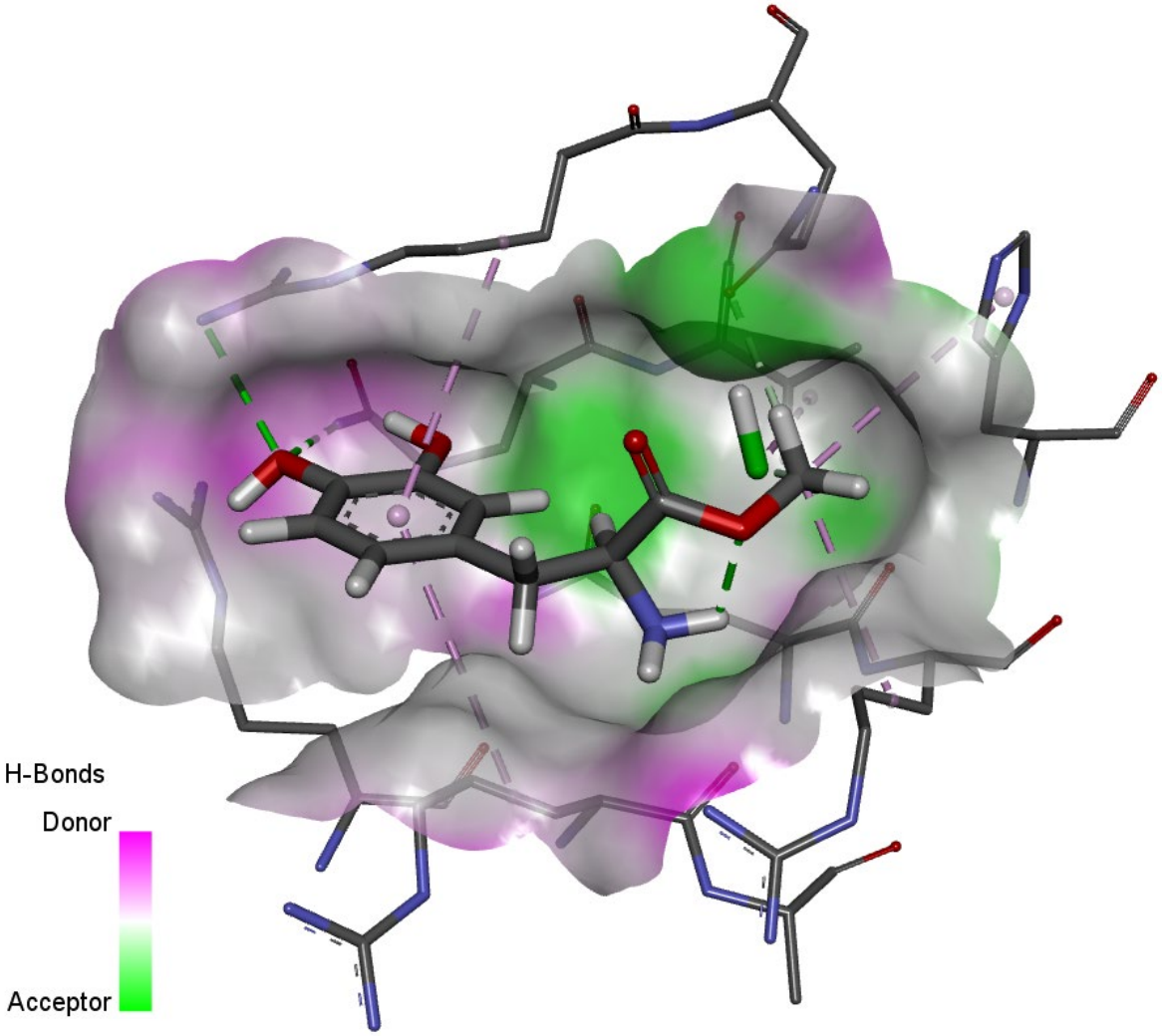

Figure. S1. The 3D form of the LDME+2DS2 interaction.

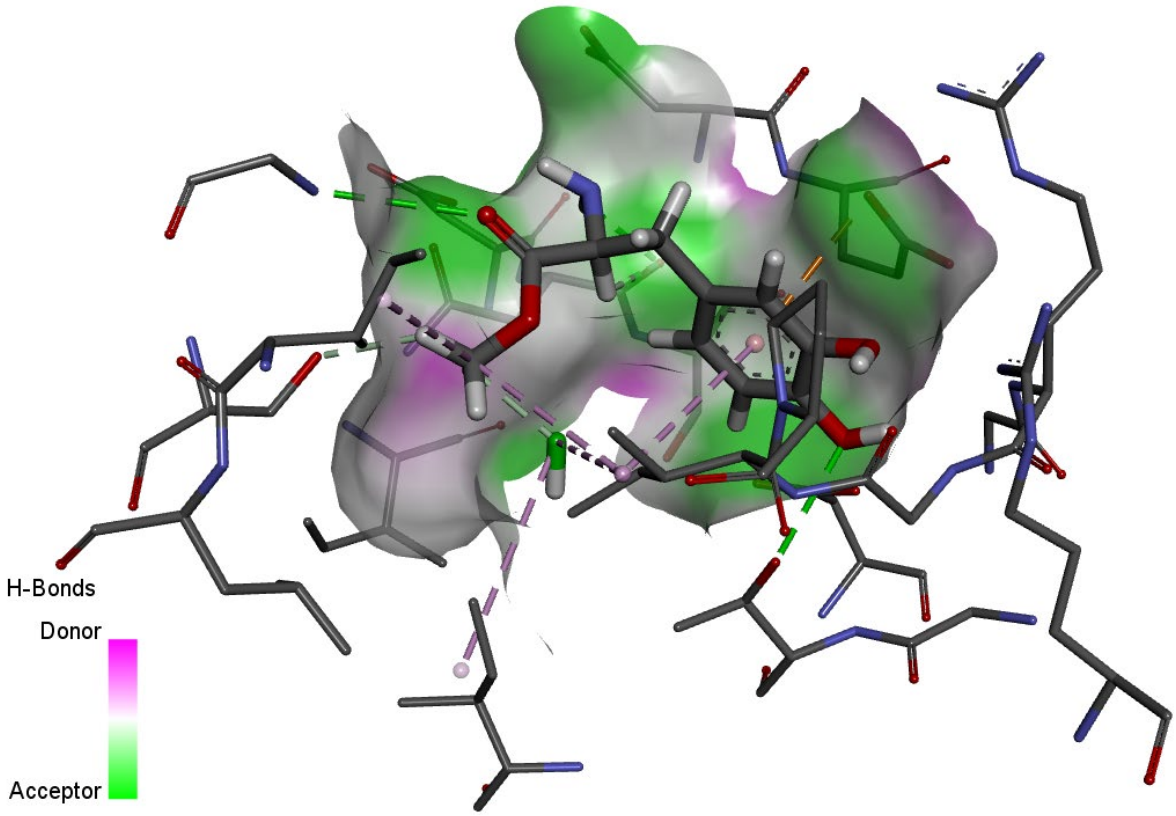

Figure. S2. The 3D form of the LDME+4URO interaction.

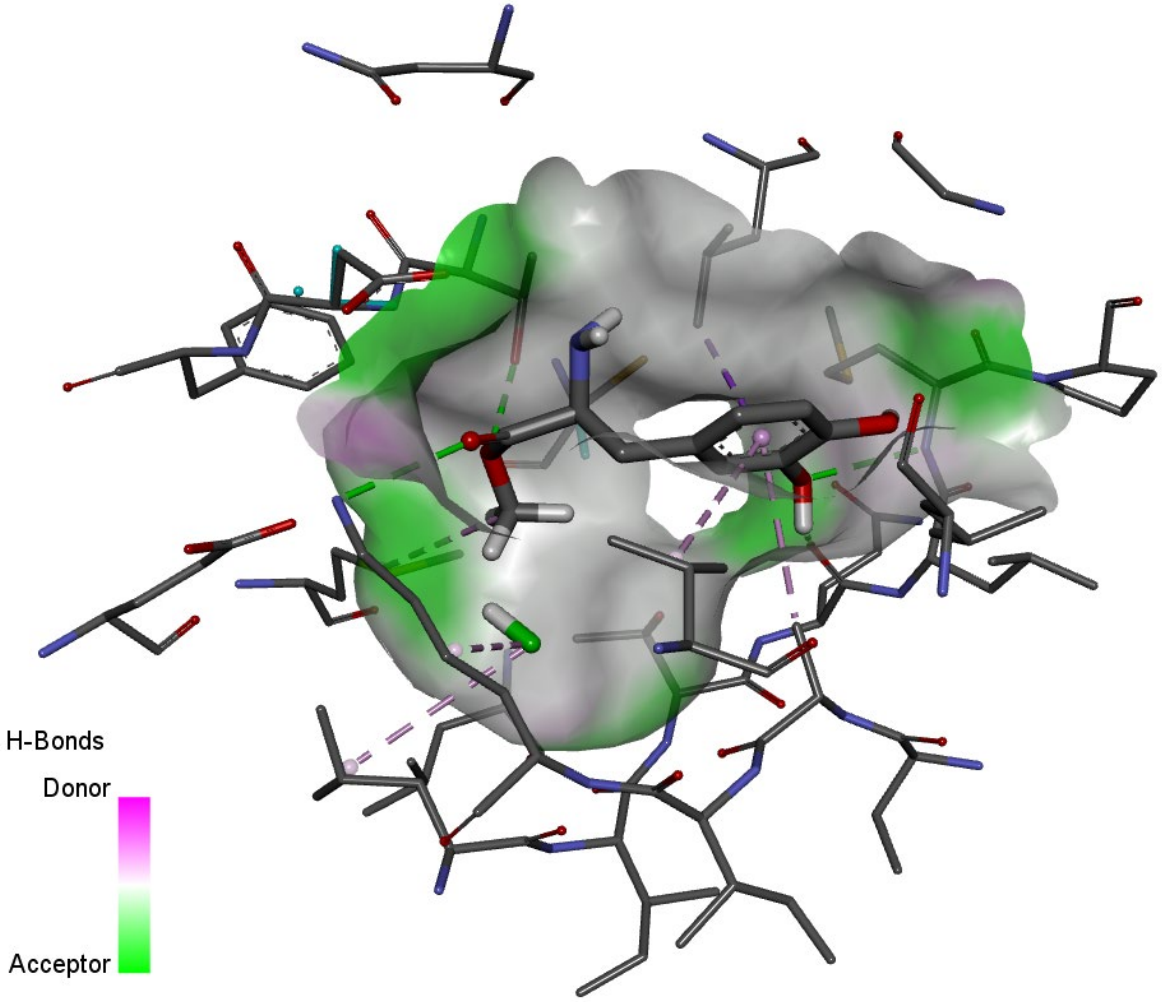

Figure. S3. The 3D form of the LDME+1M17 interaction.